BIOCHEMICAL PHARMACOLOGY 71 (2006) 872–881

available at www.sciencedirect.com

SCIENCE DIRECT®

journal homepage: www.elsevier.com/locate/biochempharm

Antioxidative function and biodistribution of $[Gd@C_{82}(OH)_{22}]_n$ nanoparticles in tumor-bearing mice

Jiangxue Wang [a,b], *Chunying Chen* [a,*], *Bai Li* [a], *Hongwei Yu* [a,b], *Yuliang Zhao* [a,**], *Jin Sun* [a,b], *Yufeng Li* [a,b], *Gengmei Xing* [a], *Hui Yuan* [a], *Jun Tang* [a], *Zhen Chen* [a], *Huan Meng* [a], *Yuxi Gao* [a], *Chang Ye* [a], *Zhifang Chai* [a], *Chuanfeng Zhu* [c], *Baocheng Ma* [c], *Xiaohong Fang* [c], *Lijun Wan* [c]

[a] *Lab for Bio-Environmental Health Sciences of Nanoscale Materials and Key Lab of Nuclear Analytical Techniques, Institute of High Energy Physics, Chinese Academy of Sciences, P.O. Box 918, Beijing 100049, PR China*
[b] *Graduate School of the Chinese Academy of Sciences, Beijing 100049, China*
[c] *Key Lab of Molecular Nanostructures and Nanotechnology, Institute of Chemistry, Chinese Academy of Sciences, Beijing 100080, China*

ARTICLE INFO

Article history:
Received 30 September 2005
Accepted 1 December 2005

Keywords:
$[Gd@C_{82}(OH)_{22}]_n$ nanoparticles
Oxidative stress
Antioxidant
Biodistribution
In vivo

Abbreviations:
CAT, catalase
CDNB, 1-chlorinechloro-2, 4-binitrobenzenedinitrobenzene
CTX, cyclophosphamide
DTNB, 5,5′-dithiobis 2-nitrobenzoic acid
GSH, glutathione
GSH-px, glutathione peroxidase
GST, glutathione S-transferase
•OH, hydroxyl radical
H_2O_2, hydrogen peroxide

ABSTRACT

Oxidative stress is considered to be one of the important mechanisms involved in carcinogenesis. In our previous study, gadolinium endohedral metallofullerenol ($[Gd@C_{82}(OH)_{22}]_n$ nanoparticles) have shown high inhibitory activity on hepatoma cell (H22) growth in mice. To explore the antioxidative functions of nanoparticles, we investigated the biodistribution of $[Gd@C_{82}(OH)_{22}]_n$ nanoparticles, the changes of blood coagulation profiles, the metabolism of reactive oxygen species (ROS) in the tumor-bearing mice as well as the possible relationships between nanoparticles treatment and ROS production in this paper. The activities of hepatic superoxide dismutase (SOD), glutathione peroxidase (GSH-Px), glutathione S-transferase (GST) and catalase (CAT) as well as the levels of reduced glutathione (GSH), protein-bound thiols and malondialdehyde (MDA) were compared between the tumor-bearing mice and normal mice. Transplanted tumors were grown in mice by subcutaneous injection of murine hepatoma cells in the mice. The comparison of the above parameters between nanoparticles and cyclophosphamide (CTX) therapy were also investigated. $[Gd@C_{82}(OH)_{22}]_n$ administration can efficiently restore the damaged liver and kidney of the tumor-bearing mice. All the activities of enzymes and other parameters related to oxidative stress were reduced after $[Gd@C_{82}(OH)_{22}]_n$ treatment and tended closely to the normal levels. The results suggest that $[Gd@C_{82}(OH)_{22}]_n$ nanoparticle treatment could regulate ROS production in vivo.

* *Corresponding author*. Tel.: +86 10 88233212; fax: +86 10 88233186.
** *Corresponding author*. Tel.: +86 10 88233191; fax: +86 10 88233191.
E-mail addresses: chenchy@mail.ihep.ac.cn (C. Chen), zhaoyuliang@ihep.ac.cn (Y. Zhao).
0006-2952/$ – see front matter © 2005 Elsevier Inc. All rights reserved.
doi:10.1016/j.bcp.2005.12.001

ICP-MS, inductively coupled plasma-mass spectrometry
MDA, malondialdehyde
NTP, 2-nitro-5-thiobenzoate anion
$^1O_2$, singlet oxygen
$O_2^{\bullet-}$, superoxide anions
PBS, phosphate buffer solution
ROS, reactive oxygen species
–SH, protein thiols
SOD, superoxidase dismutase
TBARS, thiobarbituric acid-reactive substance

1. Introduction

Fullerene, the third allotrope of carbon, was found in 1985 [1]. Because of its unique geometric structure and chemical properties, fullerenic derivatives have attracted great attention in physical, chemical, biological and medical applications. Water-soluble fullerene derivatives have not shown acute toxicity after oral administration in rats [2] and they have different affinities in vivo according to their diversity of water solubilizing groups. C_{60} derivatives could inhibit the activity of enzymes by fitting inside the hydrophobic cavity of human immunodeficiency virus (HIV) protease [3]. In vivo, ^{14}C-labeled water-miscible C_{60} was found to deposit rapidly in many tissues and to penetrate the blood–brain barrier after oral administration into rats [4]. Li et al. have found that ^{99m}Tc-$C_{60}(OH)_x$ can penetrate reticuloendothelial cells and is mainly located in bone, kidneys, spleen and liver [5]. This biological behavior of fullerenol is consistent with that of endohedral metallofullerene $^{166}Ho@C_{82}(OH)_y$ [6]. Under visible light, fullerene and its derivatives can generate singlet oxygen and exhibit a suppressive effect on tumor tissue without any damage to normal skin [7]. It has been also suggested that water-soluble fullerene derivatives could be used as a biomarker to deliver polar drugs through membranes to a target tissue. The $Gd@C_{82}(OH)_x$ has been studied as a new generation of high efficient contrast agents for magnetic resonance imaging (MRI) [8,9] and shown high efficiency for antitumor growth [10].

Oxidative stress is considered to be an important mechanism in carcinogenesis. It is a response to the abnormal metabolism of reactive oxygen species (ROS) in aerobic organisms, such as superoxide anions ($O_2^{\bullet-}$), singlet oxygen ($^1O_2$), hydrogen peroxide (H_2O_2) and hydroxyl radicals ($^{\bullet}OH$). Free radicals were involved in certain aspects of tumor growth [11,12]. They would react with all biological macromolecules and induce DNA–protein cross-links, strand breaks, base damage, lipid peroxidation and protein fragmentation [13,14].

The fullerene has been categorized as a radical sponge because it can react with free radicals in some diseases caused by a hyper-production of ROS. Carboxyfullerenes, containing three malonic acid groups per molecule, had demonstrated a potent free-radical scavenging ability in vitro and in vivo [15,16], and they exhibited excellent neuroprotective efficacy toward involvement in familial amyotrophic lateral sclerosis. Poly-hydroxylated fullerenes could effectively absorb $O_2^{\bullet-}$ generated by xanthin/xanthine oxidase [17] and scavenge hydroxyl radicals in human breast carcinoma cell lines [18]. Lai et al. proved that fullerenol diminished lipid peroxidation products and restored the glutathione (GSH) content in the small intestine after I/R injury in dogs [19]. But to our knowledge, all these for the endohedral metallofullerenol in vivo are unknown so far. More recently, we reported that gadolinium endohedral metallofullerenol ($[Gd@C_{82}(OH)_{22}]_n$ nanoparticles) have shown strong inhibition to the tumor growth with non-observable toxicity in vivo [10], though the antitumor mechanism is not clear. In this paper, the experimental results about the oxidative stress of $[Gd@C_{82}(OH)_{22}]_n$ nanoparticles in mice, the effect on blood coagulation, the production of ROS, antioxidative enzymes after treatment with $[Gd@C_{82}(OH)_{22}]_n$ nanoparticles and their biodistribution in the tumor-bearing mice are presented.

2. Materials and methods

2.1. Materials

The preparation of $[Gd@C_{82}(OH)_{22}]_n$ is the same as described in refs. [20,21], and the nanoparticle characterizations have been described in our published paper [10]. The average size of $[Gd@C_{82}(OH)_{22}]_n$ particles in saline solution was 22.4 nm (ranging from 0 to 50 nm) in diameter, which was measured by the high resolution atomic force microscopy. A Milli-Q water system (Millipore, Bedford, MA, USA) was used to prepare ultra-pure water. The reagents and kits for detecting enzyme activation were purchased from Nanjing Jiancheng Bioengineering Institute (NJBI, Nanjing, China). Bovine serum albumin and coomassie brilliant blue G-250 were purchased from Sigma. All of the other reagents used in this experiment were at least of analytical grade.

2.2. Animals and tumor inoculation

Female Kunming mice (20 ± 2 g body weight) were housed in a ventilated, temperature-controlled and standardized sterile animal room at the Cancer Institute Hospital (CIH), Chinese

Academy of Medical Sciences (CAMS). The procedures used in this experiment were conducted according to the approved protocols of the Institutional Animal Care and Use Committee of the Chinese Academy of Medical Sciences.

All of the animals were subcutaneously implanted with 1×10^6 hepatoma cells (H22) (in 100 μl saline) in the right hind leg. Before treatment, animals were randomly divided into four groups of five animals each. The design of the dosage of each group is based on our recent results [10]. One group (saline group) was given 0.9% saline intraperitoneally (i.p.), while other groups were injected i.p. with 30 mg/kg cyclophosphamide (CTX group) or 31.4 μg Gd/kg $[Gd@C_{82}(OH)_{22}]_n$ nanoparticles ($[Gd@C_{82}(OH)_{22}]_n$ group). The fourth group received i.p. injections of 31.4 μg Gd/kg $GdCl_3$ per day ($GdCl_3$ group). The dose of 31.4 μg Gd/kg $[Gd@C_{82}(OH)_{22}]_n$ nanoparticles (2×10^{-7} mol/kg) has a better inhibition rate of tumor growth in tumor-bearing mice than 1×10^{-7} mol/kg [10]. So, the high dosage of $[Gd@C_{82}(OH)_{22}]_n$ nanoparticles was selected in this experiment. Another 10 mice (normal group), as a control group, were given no treatment and only fed with normal food and water during the experiment. All three reagents were dissolved in 0.9% saline solution prior to use. Each mouse was injected with 0.2 ml solution per day from the second day of hepatoma-inoculation to the day before sacrifice. CTX, an antineoplastic agent widely used to treat patients, was only injected for the first 7 days due to its toxicity. The diameter of the tumor-loaded leg in each mouse was measured with calipers every other day. All of animals were sacrificed after being anaesthetized by aether when the diameter of the tumor-bearing leg was 2 cm in the saline group.

In addition, 20 mice were used to collect plasma for analyzing coagulation profiles. The treatment was the same as the above-mentioned procedure. Sodium citrate (3.2%) was used as anticoagulant. In the present experiment, all animals were fed with normal food and distilled water ad libitum.

2.3. Biodistribution of $[Gd@C_{82}(OH)_{22}]_n$ in tumor-bearing mice

Blood samples were collected by removing the eyeball. Serum was harvested by centrifuging blood (2500 rpm, 10 min), and red cells were kept for analyzing the Gd concentration. The skin was removed from each mouse's back, and the muscle (thigh) and bone (whole leg with marrow) were taken from the three legs without bearing tumor. The tissues and organs, such as heart, liver, spleen, kidneys, lung, thymus, uterus (ovaries), large intestine, stomach (emptied), pancreas and brain, were excised and weighed. All samples were stored at −60 °C until used.

Each tissue was weighed, digested and analyzed for Gd content. Briefly, the taken materials were soaked in nitric acid overnight and heated at about 80 °C the next day. At the same time, H_2O_2 solution was used to drive off the vapor of nitrogen oxides until the solution was colorless and clear. At last, the solution volume was fixed to 3 ml by using diluted nitric acid (concentration, 2%). Inductively coupled plasma-mass spectrometry (ICP-MS, Thermo Elemental X7, Thermo Electron Co.) was used to analyze the Gd concentration in each sample. Indium of 20 ng/ml was chosen as an internal standard element. The detection limit of Gd was 1.47 pg/ml.

2.4. Coefficients of liver, kidney and spleen

After weighing the body and tissues, the coefficients of liver, kidney and spleen to body weight were calculated as the ratio of tissue's wet weight (mg) to body weight (g).

2.5. Analyses of blood coagulation

The mice plasma was collected immediately by centrifuging whole blood at 2500 rpm for 10 min. The prothrombin time (PT), thrombin time (TT), active partial thromboplastin time (APTT) and fibrinogen (Fbg) in plasma were measured using a coagulation analyzer (SysmexCA-1500, Japan) within 2 h.

2.6. Preparation of liver extracts

A small part (0.5–1 g) of each liver sample was taken for biochemical tests. The non-tendon segments were minced with a titanium knife, washed several times by cold 0.8% NaCl buffer (0.01 mol/l Tris–HCl, 0.0001 mol/l EDTA-2Na, 0.01 mol/l sucrose, 0.8% NaCl, pH 7.4), and then homogenized at 4 °C by a triturator for 10 min. At last, the homogenates were centrifuged at 3000 rpm for 10 min. The hepatic supernatants were collected to investigate the lipid peroxidation, the activities of antioxidant enzymes and the levels of GSH and protein-bound thiols. Protein concentrations of liver extracts were determined according to the method of Bradford [22], using bovine serum albumin as the standard.

2.7. Determination of reduced glutathione and total protein-bound thiols

The levels of reduced glutathione and total–SH groups of protein in hepatic supernatant were examined using the modified method of Ellman by Sedlak et al. [23], and using commercial reduced glutathione as a standard. The levels of their thiol groups were measured at 412 nm based on the reduction of 5,5′-dithiobis 2-nitrobenzoic acid (DTNB) to 2-nitro-5-thiobenzoate anion (NTP).

2.8. Enzymatic assays

2.8.1. Glutathione peroxidase (GSH-Px)

GSH-Px activity was measured according to the modified method of Hafeman et al. [24], which was determined by monitoring the consumption of reduced glutathione under the existence of glutathione peroxidase (GSH-Px). Liver extracts, 1.0 mmol/l GSH and 0.2 mmol/l NADPH were incubated for 5 min at 37 °C. Pre-warmed H_2O_2 was added and the mixture was incubated further for 3 min exactly. At the end of 3 min, 2.0 ml buffer solution was added to the mixture, which was then centrifuged for 10 min at 3500 rpm to obtain a protein-free filtrate. The GSH in the protein-free filtrate was then determined by mixing 2.0 ml of filtrate with 2.0 ml Na_2HPO_4 and 0.5 ml of DTNB reagent. The absorbance at 412 nm was recorded. One unit was defined as a decrease of the log[GSH] of 1 μmol/min at 37 °C, while the heated samples with inactivated enzyme were used as non-enzymatic control to eliminate the interference from endogenous GSH.

2.8.2. Glutathione S-transferase (GST)

GST activity was determined by the method of Habig et al. [25]. GST can catalyze the reaction of reduced GSH and 1-chloro-2,4-dinitrobenzene (CDNB). Liver extracts were mixed with 1 ml substrate solution (1 mmol/l GSH, 1 mmol/l CDNB). The mixture was incubated for 10 min exactly at room temperature, and then 1 ml PBS buffer (100 mmol/l phosphate, pH 6.5) and 1 ml ethanol were added. After centrifugation at 3500 rpm for 10 min, the supernatants were placed on a table for 15 min after the addition of chromogenic reagent. The absorbance at 412 nm was measured and corrected for non-enzymatic reactions. One unit was defined as the decrease of the log[GSH] of 1 μmol/min at 37 °C, while the heated samples with inactivated enzyme were used as non-enzymatic control to eliminate the interference from endogenous GSH. Results were expressed as one unit per milligram protein.

2.8.3. Superoxide dismutase (SOD)

SOD activity was spectrophotometrically determined as described by Sun et al. [26]. Superoxide anion-free radicals produced by a xanthine/xanthine oxidase system can oxidize hydroxylamine into nitrous salt. Superoxide dismutase has the ability to specifically inhibit free radicals of superoxide anions and control the amount of nitrous salt. The mauve complexes formed under chromogenic reagent were determined at 550 nm. One unit of enzyme activity was defined as the amount of enzyme causing 50% inhibition in absorbance reduction of nitrous salt by superoxide dismutase per milligram protein.

2.8.4. Catalase (CAT)

CAT activity was determined by the method of adding ammonium molybdate in the reaction system [27]. Briefly, the hydrogen peroxide was catalyzed for 1 min under the existence of CAT at 37 °C, and then terminated by adding ammonium molybdate. The solutions were kept at 25 °C for 5 min and primrose stable complexes were formed by ammonium molybdate reacting with the residual H_2O_2. The CAT level can be calculated by determining the absorbance of this complex at 405 nm. One unit of enzyme activity was defined as the amount of proteins that decomposed 1 μmol H_2O_2/s. Results were expressed as one unit per milligram protein.

2.9. Lipid peroxidation of liver

The levels of lipid peroxidation expressed as malondialdehyde (MDA) were determined using the method of thiobarbituric acid reactive substances (TBARS) [28]. Liver extracts were mixed with 1 ml 10% (w/v) trichloroacetic acid, 0.8 ml ultrapure water and 1 ml 0.67% (w/v) 2-thiobarbituric acid. After vortexing, the mixtures were incubated in a boiling water bath for 45 min, and then centrifuged at 4000 rpm for 10 min. The absorbance of the supernatants at 532 nm was measured and corrected for unspecific turbidity by subtracting the absorbance at 580 nm. 0.5% TBA in 10% trichloroacetate acid was used as the blank. The concentration of MDA was expressed as nanomole per milligram protein, using 1,1,3,3-tetraethoxypropane (TEP) as the standard.

2.10. Statistical analysis

Mean and standard deviation (S.D.) were calculated for each parameter. Results were expressed as mean ± S.D. Comparisons of each group were evaluated by one-way analysis of variance (ANOVA). When the twice of S.D. is higher than the mean, non-parameter test was used to evaluate the difference. A significant difference was assumed to exist when $P < 0.05$.

3. Results

3.1. Biodistribution of $[Gd@C_{82}(OH)_{22}]_n$ nanoparticles

The concentrations of Gd in the saline group, which can be considered as the baseline values, are only several ng/g wet weight (Fig. 1). In $[Gd@C_{82}(OH)_{22}]_n$ group, the distribution of Gd in each tissue and organ are shown in Fig. 2. $[Gd@C_{82}(OH)_{22}]_n$ nanoparticles were delivered to almost all detected tissues and mainly aggregated in bone, kidneys, stomach, liver, spleen, pancreas and thymus. Except serum, red cells and brain samples, the Gd concentrations are 2–30 times higher in the $[Gd@C_{82}(OH)_{22}]_n$ nanoparticle-treated mice than the saline mice and $P < 0.05$ was observed between nanoparticle-treated and saline groups. The concentration in serum is only 1.43 ± 0.73 ng/g, similar to 1.39 ± 0.55 ng/g in the saline group (Fig. 4A). To clarify if the biodistribution observed from $[Gd@C_{82}(OH)_{22}]_n$ nanoparticles is different from metallic Gd ion itself, the biodistribution of $GdCl_3$ in mice was studied and the data were given in Fig. 3. $GdCl_3$ was distributed mainly in pancreas, bone, liver and spleen. The concentration of Gd in pancreas is 1010.21 ± 415.24 ng/g wet weight, which is two orders higher than that of $[Gd@C_{82}(OH)_{22}]_n$ group (20.33 ± 8.50 ng/g wet weight). These results suggest that the fullerene cage could not be destroyed during metabolism in organisms and the internal Gd^{3+} was not liberated and distributed to each tissue. The status of Gd in vivo represent exactly the distribution of $[Gd@C_{82}(OH)_{22}]_n$ nanoparticles.

The distributions of $[Gd@C_{82}(OH)_{22}]_n$ in the serum and brain are also expressed in the form of Gd concentrations (Fig. 4). The concentration of Gd in the brain of the $[Gd@C_{82}(OH)_{22}]_n$

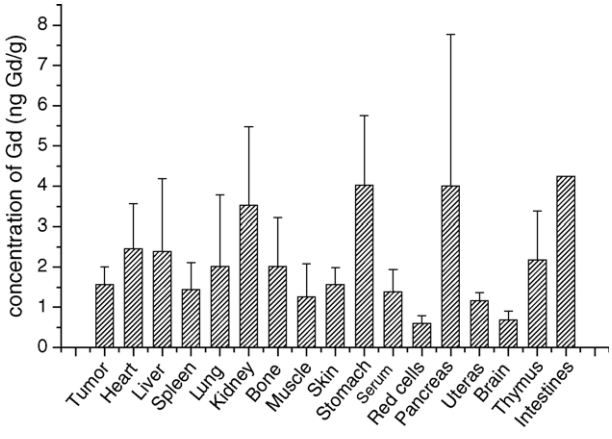

Fig. 1 – Biodistribution of Gd in the saline group (expressed as concentration of gadolinium element, ng Gd/g wet weight).

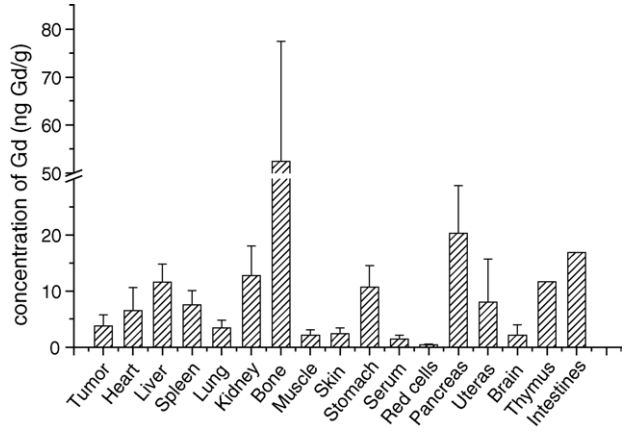

Fig. 2 – Biodistribution of $[Gd@C_{82}(OH)_{22}]_n$ nanoparticles in tumor-bearing mice (expressed as concentrations of gadolinium element, ng Gd/g wet weight).

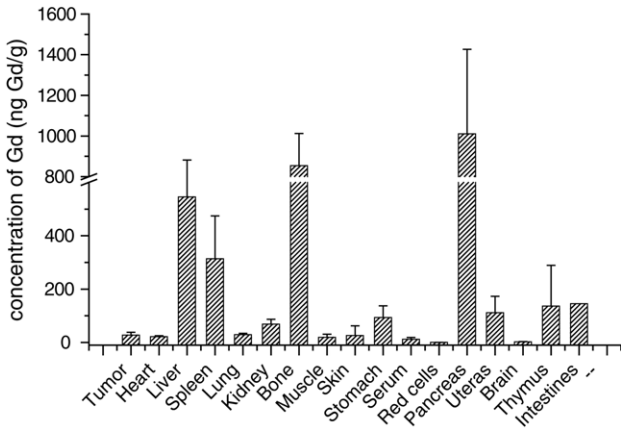

Fig. 3 – Biodistribution of $GdCl_3$ in tumor-bearing mice (expressed as concentrations of gadolinium element, ng Gd/g wet weight).

group is similar to the baseline values and lower than that in the $GdCl_3$ group, which suggested that the $[Gd@C_{82}(OH)_{22}]_n$ nanoparticles could not penetrate through the blood–brain barrier.

3.2. *Coefficients of liver, kidney and spleen*

After administration of antitumor reagents of $[Gd@C_{82}(OH)_{22}]_n$ and CTX, no abnormal behavior was found in the mice and there were no deaths. But after sacrificing these animals, big differences were found for the liver, kidneys and spleen between the nanoparticle-treated and the control mice. The coefficient of tissues to body weight is expressed as mg (tissues wet weight)/g (body weight) in Table 1.

The body weight was obviously inhibited after treatment with CTX and $[Gd@C_{82}(OH)_{22}]_n$ nanoparticles compared with the saline group because they greatly inhibited the tumor growth. After implantation of H22 hepatoma, the liver and spleen were hypertrophied obviously ($P < 0.01$) compared with the normal mice. However, after treatment with $[Gd@C_{82}(OH)_{22}]_n$ nanoparticles or CTX, the tumid symptoms decreased, although they are still higher ($P < 0.01$) than those of the normal mice. At the same time, the coefficient of kidneys is reduced significantly ($P < 0.01$) in the saline group compared with the normal level. Importantly, the kidneys damage was further deteriorated after administrating CTX because which can induce cystitis in the early stage of treatment. Contrarily, in mice treated with $[Gd@C_{82}(OH)_{22}]_n$ nanoparticles, the atrophic kidneys surprisingly recovered to the normal level.

3.3. *The effect of $[Gd@C_{82}(OH)_{22}]_n$ treatment on the coagulation profiles*

Since many tumor cells possess procoagulant activities that promote local activation of the coagulation system, variation of the coagulation cascade was examined in the present experimental tumor-bearing animals. Table 2 shows the changes of plasma PT, TT, APTT and Fbg content in the treated and untreated mice. In the $[Gd@C_{82}(OH)_{22}]_n$-treated mice, the APTT became significantly prolonged compared to the saline group, while PT was greatly reduced ($P < 0.05$). An increased Fbg content was found in plasma after injection of $[Gd@C_{82}(OH)_{22}]_n$ nanoparticles.

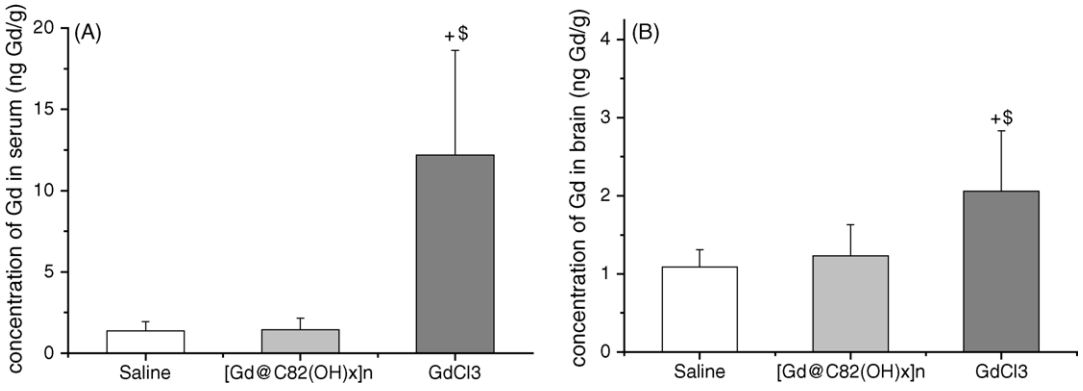

Fig. 4 – The concentrations of Gd in serum (A) and (B) brain of the saline, $[Gd@C_{82}(OH)_{22}]_n$ and $GdCl_3$ groups after 24 h of the last i.p. administration (expressed as concentrations of gadolinium element, ng Gd/g wet weight). $^{+}P < 0.01$, significantly different from the saline group; $^{\$}P < 0.01$, significantly different from the $[Gd@C_{82}(OH)_{22}]_n$ group.

Table 1 – Coefficients of liver, kidney and spleen in the tumor-bearing mice after treatment

	Saline ($n = 5$)	CTX ($n = 5$)	$[Gd@C_{82}(OH)_{22}]_n$ ($n = 5$)	Normal ($n = 10$)
Body weight (g)	32.3 ± 2.9	$27.8 \pm 2.9^{\#}$	$27.8 \pm 2.0^{\#}$	29.6 ± 2.7
Liver (mg/g)	$68.1 \pm 7.5^{**}$	$52.0 \pm 5.0^{**,+}$	$55.5 \pm 7.6^{\#,**}$	42.7 ± 3.7
Spleen (mg/g)	$9.7 \pm 2.8^{**}$	$6.0 \pm 2.1^{\#,**}$	$8.5 \pm 3.3^{**}$	3.8 ± 0.5
Kidney (mg/g)	$11.1 \pm 1.0^{**}$	$10.5 \pm 1.0^{**}$	$12.0 \pm 1.0^{\#}$	12.9 ± 1.1

Note: Results are expressed as mean ± S.D.
** $P < 0.01$, significantly different from the normal group.
# $P < 0.05$, significantly different from the saline group.
+ $P < 0.01$, significantly different from the saline group.

Table 2 – The effect of $[Gd@C_{82}(OH)_{22}]_n$ treatment on the coagulant profiles in the tumor-bearing mice

Groups ($n = 5$)	PT (s)	APTT (s)	TT (s)	Fbg (g/l)
Saline	7.96 ± 0.44	20.93 ± 3.53	7.13 ± 0.53	1.76 ± 0.11
CTX	7.87 ± 0.31	20.42 ± 2.56	7.66 ± 1.15	1.53 ± 0.37
$[Gd@C_{82}(OH)_{22}]_n$	$7.36 \pm 0.17^{\#}$	$26.36 \pm 5.55^{\#}$	7.26 ± 0.59	2.10 ± 0.37

Note: Results are expressed as mean ± S.D.
# $P < 0.05$, significantly different from the saline group.

3.4. *Oxidative stress in the liver of tumor-bearing mice*

In order to investigate the body's response to the tumor progression in vivo, several antioxidative enzymes and antioxidants were tested for mice with or without tumors. The results showed that CAT, SOD, GST ($P < 0.01$) and GSH ($P < 0.01$) in the saline group exhibited obviously higher activities than those in the normal mice (Figs. 5 and 6). The levels of protein thiols were increased, while the content of MDA marked as TBARS also showed significant elevation ($P < 0.01$) compared with the normal group (Fig. 7). The upregulated activities of enzymes could be the compensative response of the body, which suggested that the enzymes acted as a preliminary defense against the deleterious effects of increased ROS in organisms. These effects could have been initiated by the tumor inoculation and further impaired functions of liver tissue during tumor propagation.

CTX is known as an alkylating agent. Its mechanism for inhibiting tumor growth is involved in cross-linking with DNA and preventing DNA duplication, but it cannot eliminate free radicals by itself. In our study, CTX group was used as a positive control. The activities of some enzymes (CAT, SOD and GST) decreased greatly after CTX injection (30 mg/kg) compared with the saline group. However, the activities of some enzymes, such as GSH-Px, GST, SOD and GSH, were still higher ($P < 0.05$) than those in the normal mice.

CAT and GSH-Px enzymes can protect tissues from damage by consuming H_2O_2 in vivo. After treatment with $[Gd@C_{82}(OH)_{22}]_n$ nanoparticles, CAT activity in the liver was significantly downregulated ($P < 0.01$) compared with the saline group, and the activity of GSH-Px decreased too. Although, GST and SOD activities were still higher than those in normal mice, MDA and protein thiols were reduced to lower levels (Fig. 7). All these results indicate the oxidative stress status was largely regulated, and the continuous damage of tissues and liver functions were inhibited and did not further deteriorate after the injection of $[Gd@C_{82}(OH)_{22}]_n$ nanoparticles in tumor-bearing mice.

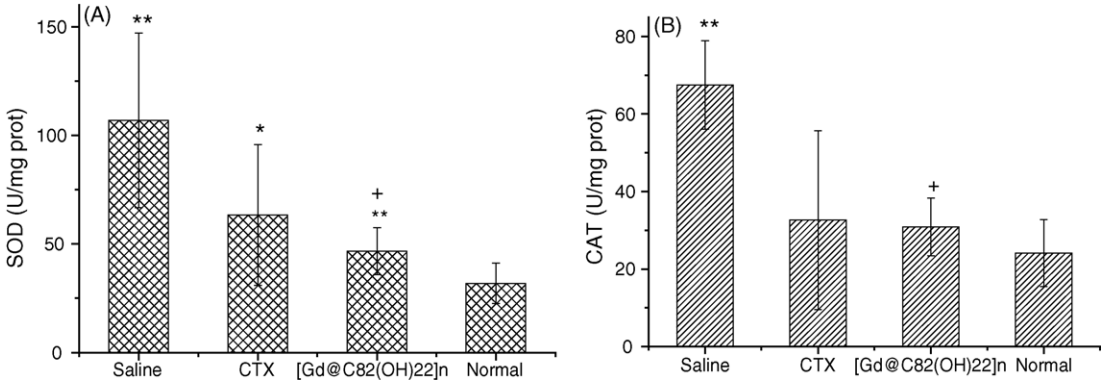

Fig. 5 – Activities of (A) superoxide dismutase (SOD) and (B) catalase (CAT) in the liver of mice treated with saline ($n = 5$), CTX (30 mg/kg, $n = 5$), $[Gd@C_{82}(OH)_{22}]_n$ nanoparticles (0.1 mmol/kg, about 31.4 μg Gd/kg, $n = 5$) and normal mice ($n = 10$). Results are expressed as mean ± S.D. $^{*}P < 0.05$ and $^{**}P < 0.01$, significantly different from the normal group; $^{+}P < 0.01$, significantly different from the saline group.

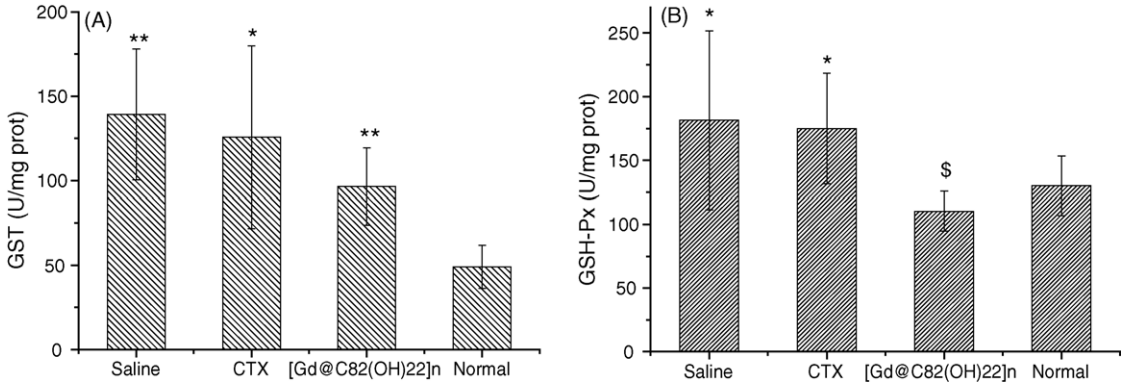

Fig. 6 – Activities of (A) glutathione *S*-transferase (GST) and (B) glutathione peroxidase (GSH-Px) in the liver of mice treated with saline (n = 5), CTX (30 mg/kg, n = 5), $[Gd@C_{82}(OH)_{22}]_n$ nanoparticles (0.1 mmol/kg, about 31.4 μg Gd/kg, n = 5) and normal mice (n = 10). Results are expressed as mean ± S.D. $^{*}P < 0.05$ and $^{**}P < 0.01$, significantly different from the normal group; $^{\$}P < 0.05$, significantly different from the CTX group.

4. Discussion

4.1. *Biodistribution*

$[Gd@C_{82}(OH)_{22}]_n$ nanoparticles mainly accumulated in bone, pancreas, spleen, kidney and liver after intraperitoneal administration and only a small quantity in the tumor and lung (Fig. 2). The concentrations in the serum and brain were very low, approximately equal to the baseline values in the saline group (Fig. 4). Though metallofullerene derivative is a kind of macromolecule with a nanoscale, the experimental data of its property in vivo are not consistent with other biomacromolecule. For instance, Watanabe et al. [29] found that the accumulation of Gd in liver was higher than that in tumor when they investigated the tumor accumulation of Gd-incorporating nanoemulsion in mice for neutron-capture

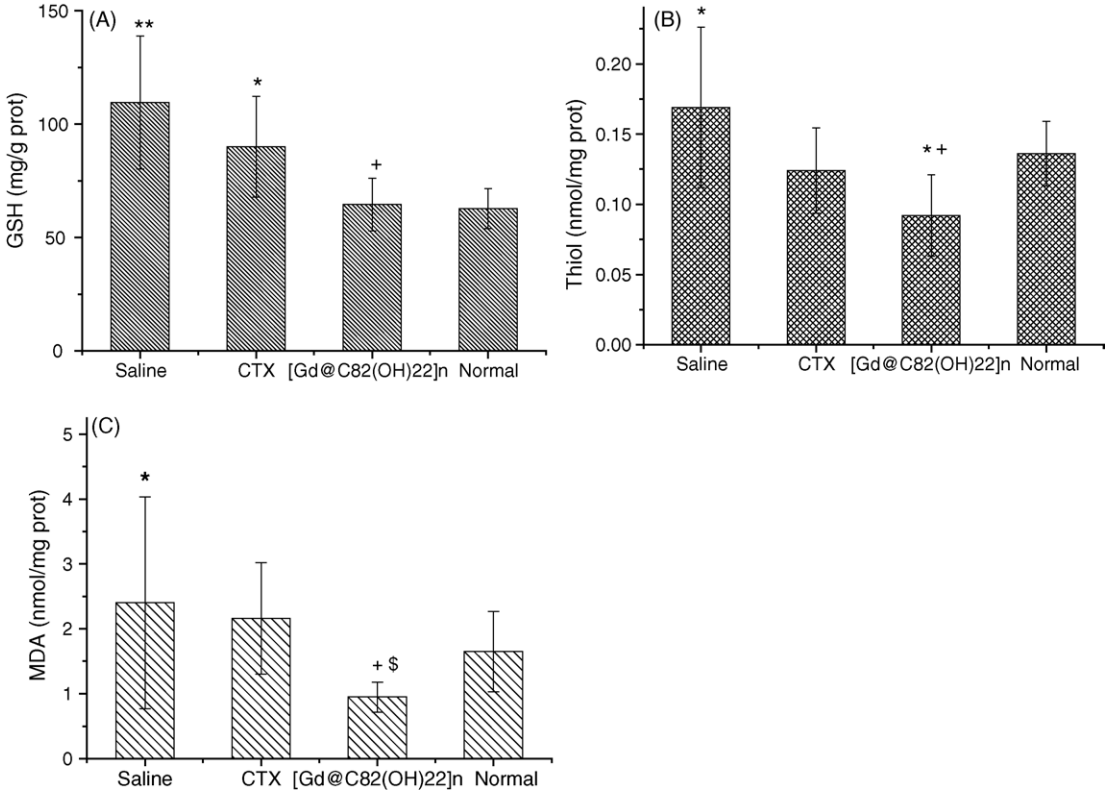

Fig. 7 – Activities of (A) reduced glutathione (GSH), (B) protein thiols (Thiols) and (C) malondialdehyde (MDA) in the liver of mice treated with saline (n = 5), CTX (30 mg/kg, n = 5), $[Gd@C_{82}(OH)_{22}]_n$ nanoparticles (0.1 mmol/kg, about 31.4 μg Gd/kg, n = 5) and normal mice (n = 10). Results are expressed as mean ± S.D. $^{*}P < 0.05$ and $^{**}P < 0.01$, significantly different from the normal group; $^{+}P < 0.01$, significantly different from the saline group.

therapy. But the present results indicated that the biodistribution of $[Gd@C_{82}(OH)_{22}]_n$ particles was quite different from the $GdCl_3$, which also suggests a high biostability of $[Gd@C_{82}(OH)_{22}]_n$ particles in vivo. $Gd@C_{82}(OH)_{40}$ was found to mainly deliver to lung, liver, spleen and kidney after intravenous administration (via tail vein) in mice [9]. As it to say, polyhydroxylated fullerene derivatives could be entrapped in the reticular–endothelial system and transported to all tissues by blood transportation in vivo, retained in the bone, liver, spleen and kidney. Moreover, Cagle et al. [6] found that $^{166}Ho@C_{82}(OH)_y$ was distributed to various tissues and organs except brain and fat quickly in 1 h after tail-vein injection, which was different from metal chelate ($Na_2[^{166}Ho(DTPA)(H_2O)]$). All these results are consistent with the present observations for biodistributions of $[Gd@C_{82}(OH)_{22}]_n$ particles.

4.2. Blood coagulation and fibrinolysis system

Activation or variation of the coagulation function existed after supplementation of $[Gd@C_{82}(OH)_{22}]_n$ compared to the untreated tumor-bearing mice. The prolongation of APTT and increased fibrinogen were observed in the $[Gd@C_{82}(OH)_{22}]_n$-treated group, and the PT was shortened (Table 2). New evidence for a strong association between cancer and coagulation has been established through detailed studies of both human and animal tumor biology. For instance, there is subclinical activation of the coagulation and fibrinolysis systems in lung cancer. Alterations in the hemostatic system are seen frequently in lung cancer correlated with the prognosis of disease [30]. A possible link with fibrinogen/fibrin and tumor growth and dissemination has been clarified using tumor-bearing fibrinogen-deficient mice [31]. The tumor cells directly or indirectly influence the coagulation system by interacting with blood cells (monocytes, platelets, neutrophils) and vascular endothelial cells. The shortened PT and increased Fbg are an indication of thrombus. Moreover, blood clotting can be accelerated not only by tissue factor also by thrombin–antithrombin (TAT) complexes. One might suspect the increased levels of TAT are induced by the changes of one or more coagulation factors within the cascades after injection of $[Gd@C_{82}(OH)_{22}]_n$ particles in the mice.

4.3. Recovery of hepatic and renal functions by nanoparticles

The function of liver (antidotal organ) and spleen of experimental mice were deteriorated because of inoculation with the H22 hepatoma, which induced the metabolic imbalance of detoxification in vivo. Surprisingly, in the $[Gd@C_{82}(OH)_{22}]_n$-treated group, the coefficients of the liver and spleen were both reduced. This indicates that the liver damage was inhibited. It is in agreement with the serum results we reported before [10], in which, the serum AST and ALT activities, the sensitive biochemical parameters for hepatocellular damage, were significantly decreased ($P < 0.01$ and $P < 0.05$ compared with the control group, respectively) by i.p. injection of $[Gd@C_{82}(OH)_{22}]_n$. But based on the changed coefficient of the kidneys, the damaged kidneys were restored to the normal level because of nanoparticle-treatments.

4.4. Antioxidant defense systems of liver enhanced by nanoparticles

As oxidative stress is considered to be an important mechanism in carcinogenesis, exploring the efficient antioxidant in vivo hence becomes one of keys for discovery of antitumor agents. The present results indicate that $[Gd@C_{82}(OH)_{22}]_n$ nanoparticle is a potential antioxidant in vivo. Possibly, this is similar with C_{60} which is characterized as a ''radical sponge'' because the multiple radicals as many as 34 methyl radicals could be added to a single C_{60} sphere.

The endogenous antioxidative system can protect organisms from the attack of free radicals. MDA, a biomarker of lipid peroxidation, reflects the degree of cell damage. In this study, the lowest MDA level was observed in $[Gd@C_{82}(OH)_{22}]_n$-treated group (Fig. 7C), whereas, the highest in saline group. Fullerene derivatives were reported to have the ability to eliminate ROS such as O^{2-}, H_2O_2, and inhibit lipid peroxidation as well. Dugan et al. [32] reported that the novel antioxidative property of carboxyfullerene derivatives rendered them as potentially neuroprotective agents against free radicals yielded by excitotoxic, apoptotic and metabolic insults in cortical cell cultures. In addition, carboxyfullerene (C_3) could interact with lipid bilayer membranes to eliminate ROS induced by transforming growth factor-β (TGF-β) and to block apoptosis signal occurred in human hepatoma Hep3B cells [33–35]. The decreased MDA level showed the reduction in free radicals and the subsequent decreased damage to the liver by $[Gd@C_{82}(OH)_{22}]_n$ nanoparticles.

Aerobic organisms possess three well-known antioxidative enzymes, i.e. GSH-Px, SOD and CAT. They are very important enzymes for their reducing H_2O_2 and superoxide radical, protecting PUFA from lipid peroxidation, and further preserving the intact structure of the cell membrane. In this study, the GSH-Px, CAT and SOD activities were downregulated after treatment with $[Gd@C_{82}(OH)_{22}]_n$ nanoparticles compared with saline group. Malonic acid derivatives of C_{60} (C_3) can imitate the biological effect of SOD to catalyze dismutation of $O_2^{\bullet-}$ [36] and they can also eliminate H_2O_2 [37]. Hydroxylated derivatives of fullerene expressed a certain scavenging activity toward $O_2^{\bullet-}$ under the existence of xanthine/xanthine oxidase [38]. Both the present results and the literature data indicate that hydroxylated fullerene derivatives are novel and potential antioxidants in vivo. $[Gd@C_{82}(OH)_{22}]_n$ nanoparticles help to keep the balance of oxidative and antioxidative systems during tumor growth in mice.

GST is a member of a family of detoxification enzymes that metabolize a variety of carcinogens by conjugating lipophilic electrophiles to GSH and is excreted out in thioether formation. In the saline group, GST activity in the liver was 139.26 ± 38.80 U/mg prot, which was 2.8 times higher than in normal mice (Fig. 6A). However, after treatment with $[Gd@C_{82}(OH)_{22}]_n$ (31.4 μg Gd/kg), GST decreased to 96.51 ± 22.93 U/mg prot indicating the reduced liver injury. The levels of GSH and protein thiols were downregulated to the normal level accompanied with reduced tumor growth (Fig. 7A and B). GSH plays a vital role in the protection of cells against oxidative stress and acts as an important water-phase non-enzymatic antioxidant and an essential cofactor for antioxidant enzymes taking part in cellular redox reactions

[39]. Its high electron-donating capacity (sulphydryl group) endows GSH with great reducing power, which is used to regulate a complex thiol-exchange system [40]. Protein thiols are also the active center of reduced GSH to eliminate free radicals by conjugating with hydroxyl radicals and superoxide anions. Their reduction in the $[Gd@C_{82}(OH)_{22}]_n$ group could be attributed to the metallofullerenol nanoparticles which possessed the ability of eliminating ROS in vivo and alleviating the burden of liver detoxification.

In general, the antioxidant enzymes significantly decline when the lipid peroxidation is elevated in carcinogenesis. It is reasonable to consider that the increased lipid peroxidation would consume more enzymes. At the meantime, increased free radicals could activate and induce the biosynthesis of antioxidative enzymes because of the compensative response in the body. This indicates that the enzyme activities and free radical could be in a dynamic balance.

In this experiment, the antioxidative systems were greatly upregulated in the tumor-bearing mice. However, after treatment with $[Gd@C_{82}(OH)_{22}]_n$, the related enzymes decreased to the lower levels. This can be attributed to the fact that $[Gd@C_{82}(OH)_{22}]_n$ nanoparticles can efficiently inhibit the tumor growth [10] and scavenge excessive free radicals during tumor growth. Nevertheless, a thorough understanding of the pathway needs lots of further investigation.

In conclusion, after inoculation of H22 hepatoma in normal mice, the coefficients of the liver and spleen and the antioxidative enzymes activities increased significantly. This phenomenon suggests that the adaptive response of the redox-defense systems in the liver could be an auto-protective mechanism in vivo. But after treatment with $[Gd@C_{82}(OH)_{22}]_n$ nanoparticles, these parameters was reduced to a lower level. The results indicate that the $[Gd@C_{82}(OH)_{22}]_n$ can produce antitumor activity via helping to recover hepatic and renal functions and regulate oxidative stress in tumor cells. Furthermore, the present results imply that some appropriate modifications to the unique surface of fullerene cages (with an appropriate nanosized particles) may lead to new ways for potential biomedical applications, such as drug carriers, drug delivery, disease diagnoses or therapy.

Acknowledgements

This study is financially supported by the Chinese National Natural Science Foundation (10490180, 90406024 and 20571076), the National Science Fund for Distinguished Young Scholars (10525524), the Ministry of Science and Technology (2005CB724703), the major directionary program of the Chinese Academy of Sciences and the National Center for Nanosciences and Nanotechnology of China.

REFERENCES

[1] Kroto HM, Heath JR, O'Brien SC, Curl RF, Smalley RE. C60: Buckminsterfullerene. Nature (London) 1985;318:162–3.
[2] Chen HH, Yu C, Ueng TH, Chen S, Chen B, Huang KJ, et al. Acute and subacute toxicity study of water-soluble polyalkysulfobated C60 in rats. Toxicol Pathol 1998;26(1):143–51.
[3] Friedman SH, DeCamp DL, Sijbesma RP. Inhibition of the HIV-1 protease by fullerene derivatives: model building studies and experimental verification. J Am Chem Soc 1993;115:6506–9.
[4] Yamago S, Tokuyama H, Nakamura E, Kikichi K, Kananishi S, Sueki K, et al. In vivo biological behavior of a water-miscible fullerene: 14C labeling, absorption, distribution, excretion and acute toxicity. Chem Biol 1995;2:385–9.
[5] Li QN, Xiu Y, Zhang XD, Liu RL, Du QQ, Shun XG, et al. Preparation of ^{99m}Tc-$C_{60}(OH)_x$ and its biodistribution studies. Nucl Med Biol 2002;29:707–10.
[6] Cagle DW, Kennel SJ, Mirzadeh S, Alford JM, Wilson LJ. In vivo studies of fullerene-based materials using endohedral metallofullerene radiotracers. Proc Natl Acad Sci USA 1999;96:5182–7.
[7] Tabata Y, Murakami Y, Ikada Y. Photodynamic effect of polyethylene glycol-modified fullerene on tumor. Jpn J Cancer Res 1997;88:1108–16.
[8] Bolskar RD, Benedetto AF, Husebo LO, Price RE, Jackson EF, Wallace S, et al. First soluble M@C60 derivatives provide enhanced access to metallofullerenes and permit in vivo evaluation of $Gd@C_{60}[C(COOH)_2]_{10}$ as a MRI contrast agent. J Am Chem Soc 2003;125:5471–8.
[9] Mikawa M, Kato H, Okumura M, Narazaki M, Kanazawa Y, Miwa N, et al. Paramagnetic water-soluble metallofullerenes having the highest relaxivity for MRI contrast agents. Bioconjug Chem 2001;12:510–4.
[10] Chen CY, Xing GM, Wang JX, Zhao YL, Li B, Jia G, et al. Multihydroxylated $[Gd@C_{82}(OH)_{22}]_n$ nanoparticles: antineoplastic activity of high efficiency and low toxicity. Nano Lett 2005;5(10):2050–7.
[11] Goldstein BD, Czerniceki B, Witz G. The role of free radicals in tumor promotion. Environ Health Perspect 1989;81:55–7.
[12] Navarro J, Obrador E, Carretero J, Petschen I, Avino J, Perez P, et al. Changes in glutathione status and the antioxidant system in blood and in cancer cells associate with tumor growth in vivo. Free Radic Biol Med 1999;26:410–8.
[13] Ahsan H, Ali A. Oxygen free radicals and systemic autoimmunity. Clin Exp Immunol 2003;131:398–404.
[14] Lloyd RV, Hanna PM, Mason RP. The origin of the hydroxyl radical oxygen in the Fenton reaction. Free Radic Biol Med 1997;22:885–8.
[15] Dugan LL, Turetsky DM, Du C, Lobner D, Wheeler M, Almli CR, et al. Carboxyfullerenes as neuroprotective agents. Proc Natl Acad Sci USA 1997;94:9434–9.
[16] Wang C, Tai LA, Lee DD, Kanakamma PP, Shen CKK, Luh TY, et al. C60 and water-soluble fullerene derivatives as antioxidants against radical-initiated lipid peroxidation. J Med Chem 1999;42:4614–20.
[17] Chiang LY, Wang LY, Swirzewski JW, Soled S, Cameron S. Efficient synthesis of polyhydroxylated fullerene derivatives via hydrolysis of polycyclosulfated precursors. J Org Chem 1994;59:3960–8.
[18] Puhaca B. In vitro modulation of adriamycin-inducaed cycotoxicity of fullerol $C_{60}(OH)_{24}$. Med Pregl 1999;52(11–12):521–6.
[19] Lai HS, Chen WJ, Chiang LY. Free radical scavenging activity of fullerenol on the ischemia-reperfusion intestine in dogs. World J Surg 2000;24:450–4.
[20] Tang J, Xing GM, Yuan H, Cao WB, Jing L, Gao XF, et al. Tuning electronic properties of metallic atom in bondage to a nanospace. J Phys Chem B 2005;109:8779–85.
[21] Xing GM, Zhang J, Zhao YL, Tang J, Zhang B, Gao XF, et al. Influences of structural properties on stability of fullerenols. J Phys Chem B 2004;108:11473–9.
[22] Bradford MM. A rapid and sensitive method for the quantitation of microgram quantities of protein utilizing

the principle of protein-dye binding. Anal Biochem 1976;72:248–54.
[23] Sedlak J, Lindsay RH. Estimation of total, protein-bound, and nonprotein sulfhydryl group in tissue with Ellman's reagent. Anal Biochem 1968;25:192–205.
[24] Hafeman DG, Sunde RA, Hoekstra WG. Effect of dietary selenium on erythrocyte and liver glutathione peroxidase in the rat. J Nutr 1974;104:580–7.
[25] Habig WH, Pabst MJ, Jakoby WB. Glutathione S-transferases: the first enzymatic step in mercapturic acid formation. J Biol Chem 1974;249:7130–9.
[26] Sun Y, Oberley LW, Li Y. A simple method for clinical assay of superoxide dismutase. Clin Chem 1988;34(3):497–500.
[27] Goth L. A simple method for determination of serum catalase activity and revision of reference range. Clin Chim Acta 1991;196:143–51.
[28] Dahle LK, Hill EG, Holman RT. The thiobarbituric acid reaction and the autoxidants of polyunsaturated fatty acid methyl esters. Arch Biochem Biophys 1962;98:253–61.
[29] Watanabe T, Ichikawa H, Fukumori Y. Tumor accumulation of gadolinium in lipid-nanoparticles intravenously injected for neutron-capture therapy of cancer. Eur J Pharm Biopharm 2002;54:119–24.
[30] Ünsal E, Atalay F, Atikcan S, Yilmaz A. Prognostic significance of hemostatic parameters in patients with lung cancer. Respir Med 2004;98(2):93–8.
[31] Degen JD, Palumbo JS. Mechanisms linking hemostatic factors to tumor growth in mice. Pathophysiol Haemost Thromb 2003;33(Suppl. 1):31–5.
[32] Dugan LL, Lovett EG, Quick KL, Lotharius J, Lin TT, O'Malley KL. Fullerene-based antioxidants and neurodegenerative disorders. Parkinsonism Relat Disord 2001;7:243–6.
[33] Huang YL, Shen CKF, Luh TY, Yang HC, Hwang KC, Chou CK. Blockage of apoptotic signaling of transforming growth factor-β in human hepatoma cells by carboxyfullerene. Eur J Biochem 1998;254:38–43.
[34] Frein D, Schildknecht S, Bachschmid M, Ullrich V. Redox regulation: a new challenge for pharmacology. Biochem Pharmacol 2005;70(6):811–23.
[35] Wang C, Tai LA, Lee DD, Kanakamma PP, Shen CKK, Luh TY, et al. C60 and water-soluble fullerene derivatives as antioxidants against radical-initiated lipid peroxidation. J Med Chem 1999;42:4614–20.
[36] Ali SS, Hardt JI, Quick KL, Kim-Han JS, Erlanger BF, Huang TT, et al. A biologically effective fullerene (C60) derivative with superoxide dismutase mimetic properties. Free Radic Biol Med 2004;37(8):1191–202.
[37] Dugan LL, Turetsky DM, Du C, Lobner D, Wheeler M, Almli CR, et al. Carboxyfullerenes as neuroprotective agents. Proc Natl Acad Sci USA 1997;94:9434–9.
[38] Mirkova SM, Djordjevicc AN, Andricb NL, Andricb SA, Kosticb TS, Bogdanovicd GM, et al. Nitric oxide-scavenging activity of polyhydroxylated fullerenol $C_{60}(OH)_{24}$. Nitric Oxide 2004;11:201–7.
[39] Sies H. Glutathione and its role in cellular functions. Free Radic Biol Med 1999;27:916–21.
[40] Dickinson DA, Forman HJ. Cellular glutathion and thiols metabolism. Biochem Pharmacol 2002;64:1019–26.